journal

J. Am. Ceram. Soc., **91** [5] 1646–1652 (2008)
DOI: 10.1111/j.1551-2916.2008.02334.x

Low Friction in CuO-Doped Yttria-Stabilized Tetragonal Zirconia Ceramics: A Complementary Macro- and Nanotribology Study

Ewa Tocha,[‡] Henry R. Pasaribu,[§] Dik J. Schipper,[§] Holger Schönherr,[†,‡] and G. Julius Vancso[†,‡]

[‡]Department of Materials Science and Technology of Polymers, MESA$^+$ Institute for Nanotechnology and Faculty of Science and Technology, University of Twente, 7500 AE Enschede, The Netherlands

[§]Laboratory for Surface Technology and Tribology, IMPACT Institute of Mechanics, Faculty of Engineering Technology, Processes and Control, University of Twente, 7500 AE Enschede, The Netherlands

The tribological behavior of CuO-doped yttria-stabilized tetragonal zirconia (3Y-TZP) ceramics in the absence of additional lubricants was characterized by macroscale pin-on-disk measurements and nanoscale atomic force microscopy (AFM) for a broad range of velocities. The previously observed low shear strength interfacial layers generated in pin-on-disk tracks by Al_2O_3 ball counter surfaces on CuO-doped 3Y-TZP, as well as virgin surfaces, were probed quantitatively by AFM with Si_3N_4 tips as the counter surface. The observed trends in nanoscale coefficient of friction determined by AFM were found to be in agreement with data acquired using a pin-on-disk tribometer. The combined data support the notion that a layer of surface contaminations is removed during the initial sliding, and wear of high asperities occurs. Subsequently, an interfacial layer with low shear strength is generated during sliding. While these results do not provide an exhaustive explanation for the process of layer formation, they represent the first report of bridged nano- and macrotribological analysis of a compositionally heterogeneous low-friction, low-wear ceramic material and further confirm some of the key assumptions for the deterministic model reported previously by Pasaribu and Schipper.

I. Introduction

FRICTION and wear play a crucial role in the application of ceramics in the absence of lubricants under dry sliding conditions. In general, it has been established that plastic deformation of asperities, lateral forces to move debris particles, viscous forces, and ploughing terms contribute to the friction force observed.[1] To understand the complex behavior of real contacts and to ultimately be able to design high-performance materials based on first principles, it is desirable to learn about the properties of single asperity interfacial friction and the energy dissipation at the fundamental level.[2,3] Based on this understanding and, among others, the understanding of plastic deformation of small asperities, multiasperity friction and the role of different mechanisms can be addressed.

Until now, it was practically impossible to bridge the various length and times scales between nanotribology and macrotribology due to technical and instrumental limitations.[4] Recently, these shortcomings have been in parts successfully overcome by the development of a high-velocity atomic force microscopy (AFM) setup and the introduction of a reliable, generally applicable calibration strategy that allow one to acquire previously unattainable nanoscale friction data.[5,6]

For technological applications, materials that exhibit a low coefficient of friction (≤ 0.2) and high wear resistance (wear rate $< 10^{-6}$ mm$^3 \cdot$(N $\cdot$ m)$^{-1}$) are required.[7] Liquid lubrication (mainly based on organic materials) is the most widely used method to reduce interfacial shear strength, resulting in low-friction systems.[8] However, for some applications, such as those in high temperatures, in a cryogenic environment, and in high vacuum, liquid lubricants do not function properly or can be a source of contamination.[9] In these applications, dry sliding is used. Here, friction can be reduced by creating a weak interface between two opposing surfaces (made of a hard material) that supports the normal load. This can be realized using a thin layer of soft material (solid lubricant) to provide easy shear.[10] Solid lubrication is obtained either by covering the surface with a thin layer of soft material (graphite, MoS_2, and CF_x)[11–16] or by a self-lubricating composite,[17,18] in which a second phase composed of soft particles is embedded in the base material. Owing to the high contact pressure during sliding, a soft interfacial layer is generated. The frictional behavior of such layered systems depends critically on the thickness of the layer formed. When the layer is very thin, the interaction between the opposing surfaces is dominated by the contact of the asperities of the counter surface with the substrate of the composite; thus, the coefficient of friction is equivalent to the value for the substrate without the layer. For very thick layers, the coefficient of friction is determined by the bulk properties of the layer material generated.

Self-lubricating composites have been reported for metals and ceramics.[18–21] A reduction of friction was observed for instance for alumina and zirconia systems doped with CuO sliding against alumina.[17,22,23] The experimental results showed that addition of 8 mol% of CuO to tetragonal zirconia stabilized with 3 mol% yttria-stabilized tetragonal zirconia (3Y-TZP) reduced the coefficient of friction from ~ 0.7 to ≤ 0.3. Combined transmission electron microscopy and energy-dispersive X-ray analyses of the doped 3Y-TZP revealed crystalline zirconia grains several hundred nanometers in diameter and crystalline Cu-rich phases among the zirconia grains. Nanoindentation tests performed on the wear tracks where a low friction was observed showed a significantly reduced hardness of 6 GPa as compared with the bulk value of 14 GPa.[22,24]

To explain these results, Pasaribu and Schipper[25] proposed a friction model for layered systems based on a deterministic contact model. In this model, the rough surface is represented by a distribution of spherically shaped asperities with different radii and heights (Scheme 1). The contributions of both adhesion and ploughing toward friction are taken into account by a summation of the resistance to motion experienced by each asperity in elastic, elastic—plastic, and plastic contact. Using this model, the value of the macroscopic coefficient of friction can be successfully predicted for a known (or assumed) thickness of the soft layer and the fractional surface coverage of the generated

R. Scattergood—contributing editor

Manuscript No. 23882. Received October 18, 2007; approved January 18, 2008.
This work was financially supported by the Dutch Technology Foundation STW (STW-project 5287, Nanoscale wear-resistant ceramic materials with low friction) and the European Office of Aerospace Research & Development (EOARD) of US-AF.
[†]Author to whom correspondence should be addressed. e-mails: h.schonherr@tnw.utwente.nl, g.j.vancso@tnw.utwente.nl

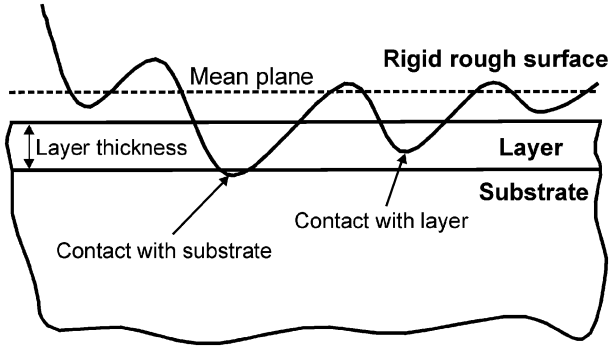

Scheme 1. Schematic of the soft layer and different types of contact in a multiasperity contact.

interfacial layer on the wear track. This model led to *quantitative* agreement with the experimental data. Even though the model can successfully predict the macroscopic coefficient of friction, the mechanism responsible for the formation of this layer and the nature and some properties of this soft layer remain unknown to date.

To obtain a better understanding of the processes that occur during sliding of an alumina ball against CuO-doped 3Y-TZP ceramics, the wear tracks obtained in such macrotribological experiments were studied by AFM for various sliding distances. In addition, the nanotribological behavior of the wear track and in particular the layer formed in the pin-on-disk measurements were investigated for a broad range of scanning velocities, thus aiming at bridging across the length and time scales of nano- and macrotribology.

II. Experimental Procedure

(1) Materials and Sample Preparation

Ninety-four percent to 95% dense 3Y-TZP samples (doped with 8 mol% CuO) were obtained from Dr. S. Ran and Dr. A. J. A. Winnubst (IMS group, University of Twente, the Netherlands). Appropriate amounts of 3Y-TZP (TZ3Y, Tosoh, Tokyo, Japan) and CuO (Aldrich, Steinheim, Germany) powders were mixed by wet milling using ethanol (Biosolve, Westford, MA). After drying, green compact disks were prepared by uniaxial pressing at 30 MPa, followed by isostatic pressing at 400 MPa. These disks were sintered for 8 h in stagnant air at 1500°C. The heating and cooling rates used during sintering were both 2°C/min. The sintered disks were polished to a centerline surface roughness (R_a) of 0.1 μm using diamond paste. The polished disks were ultrasonically cleaned in ethanol and then annealed at 850°C for 2 h. A detailed description of the sample preparation can be found in Pasaribu and colleagues[22,26] and Ran *et al.*[27]

(2) Pin-on-Disk Measurements

Macrotribology experiments were performed using a pin-on-disk tribometer (Tribometer, CSEM, Neuchâtel, Switzerland). The instrument was placed in a climate chamber (HC4057, Heraeus, Balingen, Germany) to maintain constant testing conditions (40% relative humidity (RH)). Sliding tests were conducted with a load of 5 N (unless differently specified) and a velocity of 0.05 m/s for different sliding distances (up to 450 m). Commercially available 10-mm-diameter α-Al_2O_3 balls (GIMEX Technische Keramiek BV, Geldermalsen, the Netherlands) with a grain size of 0.1–0.3 μm, and 10-mm-diameter Si_3N_4 balls (HPSN, GIMEX Technische Keramiek BV) were used as the counter surface. The data agreed to within the experimental error with previously reported data acquired on multiple specimens prepared using the same protocols.[22–27]

Before the pin-on-disk measurements, the samples and the balls were ultrasonically cleaned for 30 min in ethanol (99.8% purity, Biosolve) and subsequently annealed for 20 min at 120°C.

(3) Nanotribology

Following the pin-on-disk studies, the nanotribology of the tracks generated in the macrotribology tests was investigated using AFM without further surface treatment, i.e. the tracks generated were directly analyzed. The data were acquired in different sample orientations (i.e., effective tip scan directions) relative to the direction of the wear track to confirm that the relative scan angle did not influence the friction data. Some samples were additionally treated by oxygen-plasma (30 mA, 60 mTorr) using a Plasma Prep II (SPI Supplies, West Chester, PA) for 10 min.

Friction force measurements were performed using a NanoScope Multimode IIIa atomic force microscope (Digital Instruments/Veeco, Santa Barbara, CA) enclosed in a homebuilt glovebox. The normal spring constants ($k_N = 0.20$–0.22 N/m) of "V"-shaped Si_3N_4 cantilevers (Model NP, Veeco Nano Probe, Santa Barbara, CA; silicon-rich silicon nitride deposited by chemical vapor deposition) and tip radii (in the range of 40–70 nm) were individually calibrated using the reference lever method[28] and a calibration grating (silicon grating TGT1, NT-MDT, Moscow, Russia). The RH of 40% ± 2% was precisely controlled using a mixture of wet and dry N_2 gas, as measured by a humidity sensor (SHT15, Sensirion, Zurich, Switzerland), while the temperature was maintained constant during all measurements (25°C). Friction data in the form of images of differential photodiode output signals for trace and retrace scans (512 × 128 pixels; scan size 1000 nm × 250 nm; scan velocity 6.1 μm/s) were acquired simultaneously for different normal forces (normal force is defined as the sum of pull-off force and an externally applied load). The normal forces were limited to values <100 nN to ensure that the data were captured in the elastic contact regime without detectable tip wear.[29,30] Subsequent to a correction of the scanner hysteresis between trace and retrace using the Digital Instruments software, the mean friction force ± standard deviation σ was determined from an analysis of difference images, as described in Hammerschmidt *et al.*[31] The friction force data were calibrated according to the wedge method.[5,32,33]

Coefficient of friction velocity measurements (scan size of 250 nm) were performed with a stand-alone AFM (Pico-SPM, Molecular Imaging, Tempe, AZ) equipped with the newly developed high-velocity accessory, described in detail in Tocha *et al.*[6] The lateral photodiode output signal, which was acquired in the time domain, was recorded via a data acquisition board and was processed by the custom-made software. Each data point represents the mean value of one-half of the difference friction signal calculated from 150 trace and retrace cycles, and the error bars correspond to the standard deviation of the data analyzed for a given load and velocity. The climate control (40% ± 2% RH and temperature 25°C) was performed via the flow of nitrogen gas of controlled humidity through an environmental chamber (PicoAPEX, Molecular Imaging) as measured by a humidity sensor (SHT15, Sensirion, Zurich, Switzerland).

III. Results and Discussion

The study reported below was focused on the quantitative characterization of the macro- and nanotribological behavior of the soft layer formed in the wear tracks between an α-Al_2O_3 ball and CuO-doped 3Y-TZP.[22,26] The narrowing of the gap of experimental length and time scales will allow a direct comparison of the data obtained in pin-on-disk and AFM tribology measurements and thereby help to unravel new insight required to confirm and improve recently developed models for solid lubrication under dry sliding conditions.[25,34]

(1) Macrotribology of 3Y-TZP Doped with CuO

The macrotribological behavior as well as the formation of the soft layer of CuO-doped 3Y-TZP samples were investigated using an α-Al_2O_3 ball in a pin-on-disk tribometer. Different

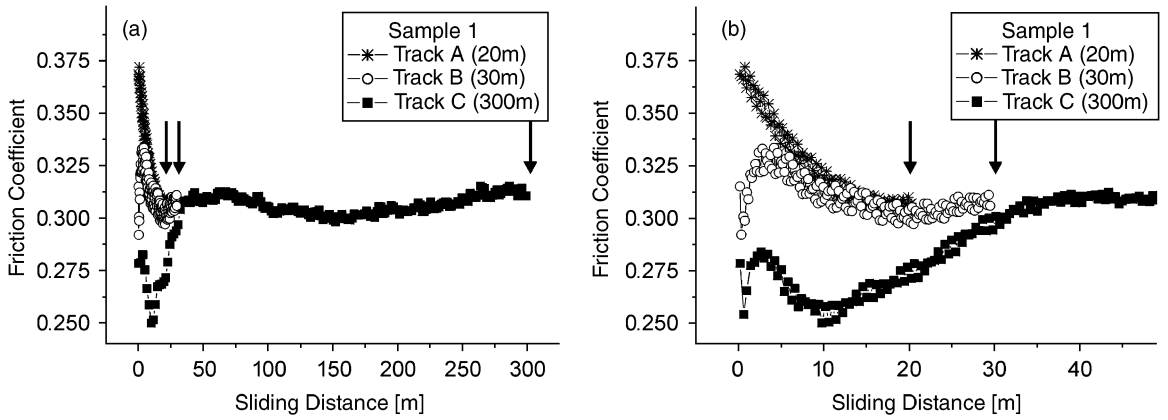

Fig. 1. Coefficient of friction as a function of sliding distance for a yttria-stabilized tetragonal zirconia (3Y-TZP) sample doped with 8 mol% CuO measured against an α-Al_2O_3 ball using a pin-on-disk tribometer (normal load 5 N, velocity 5×10^4 μm/s, 40% RH, 25°C). Plot (b) shows a magnified section of (a) showing the coefficient of friction for the initial sliding distances. The arrows mark the end of each of these experiments. RH, relative humidity.

tracks were generated for various sliding distances representing different stages of the layer formation. Figure 1 shows the measured coefficient of friction as a function of sliding distance for various tracks. The pin-on-disk measurements on sample 1 were conducted (in separate tracks) for 20, 30, and 300 m; the tracks thus generated were labeled tracks A, B, and C.

The initial value of the friction coefficient on CuO-doped 3Y-TZP $\mu^{macro}_{\alpha\text{-}Al_2O_3}$ (the subscript denotes the chemical composition of the counter surface, the superscript denotes the method of testing: pin-on-disk (macro) or AFM (nano)) varied approximately between 0.25 and 0.35, and after sliding for 100 m the coefficient of friction reached a steady-state value of approximately 0.30–0.40. The initially low value of $\mu^{macro}_{\alpha\text{-}Al_2O_3}$ is attributed to the presence of contaminations resulting in lubrication of the contacting surfaces. Cleaning with ethanol and temperature treatment only partly removes a contamination layer from the surface. These carbon-containing contaminations and their removal were detected in independent X-ray photoelectron spectroscopy (XPS) imaging measurements (Supporting Information, Figure S1). The initial part of the plot was observed to be somewhat different for various nominally identical samples, which is attributed to variations in the contamination layer. However, for all samples, the steady-state value of $\mu^{macro}_{\alpha\text{-}Al_2O_3}$ was reached after sliding for 100 m. As compared with the pure 3Y-TZP system ($\mu^{macro}_{\alpha\text{-}Al_2O_3}$ (3Y-TZP) = 0.7),[22] a significant reduction in the coefficient of friction was observed. In Pasaribu *et al.*[22], the authors reported that the surface of CuO-doped 3Y-TZP was deformed plastically during sliding and that an interfacial layer was generated in the contact area.[35] The low-friction behavior was associated with the presence of this layer, which was shown to possess significantly lower hardness ($H \cong 6$ GPa) than the bulk sample ($H \cong 14$ GPa).

In order to provide a basis for comparison of the nano- and macrotribology in this study, a CuO-doped 3Y-TZP sample was first probed with an α-Al_2O_3 ball (to generate the soft interfacial layer) and then on the same track with a ball made of Si_3N_4, which is the typical AFM tip material (Fig. 2). In this experiment, the coefficient of friction of the Si_3N_4 slider ($\mu^{macro}_{Si_3N_4}$) maintained the same value as the α-Al_2O_3 slider during the first several meters of sliding. After sliding for a distance of *ca.* 4 m, the coefficient of friction increased rapidly. This increase in $\mu^{macro}_{Si_3N_4}$ coincided with the onset of severe wear of the ball, as also detected by visual inspection using an optical microscope. Direct wear-less testing of 3Y-TZP/CuO with a Si_3N_4 ball was impossible as severe wear was observed for all sliding distances and loads. Based on the observation of the constant coefficient of friction on the first meters of sliding of the Si_3N_4 ball, we assume that $\mu^{macro}_{Si_3N_4}$ and $\mu^{macro}_{\alpha\text{-}Al_2O_3}$ measured on the wear track are very similar (in the absence of wear).

(2) Nanotribology of 3Y-TZP Doped with CuO

In contrast to the multiasperity contact in the pin-on-disk experiments discussed above, AFM nanotribological measurements may afford an insight into tribological processes on the single asperity level. Low-magnification AFM height images (no data shown) provided evidence for the formation of an elevated layer in the wear track. Besides the locally resolved differences in tribological behavior by AFM, attention was focused on quantitatively analyzing the tribological behavior of selected areas in the wear track.

Simultaneous mapping of topography and friction force revealed that the wear tracks showed an inhomogeneous friction on the nanometer scale in some areas (see Fig. 3). Higher friction forces were measured in depressions whereas smooth areas showed low friction forces. Most likely, this result is a consequence of local variations in the tip-sample interface caused by variable film thickness of the layer formed in the wear track. Whereas areas with a thicker film already showed the described effect of this soft layer, the areas that appeared lower in height in AFM images did not yet lead to a reduction of friction as the soft layer here was presumably too thin or absent.

Further nanotribological analyses were performed on the flat areas, which did not show pronounced contrast in friction force maps for a given load (Fig. 4). These smooth regions of the ceramic, which are characterized by a root-mean-square roughness smaller than 6 nm assessed by AFM on scan sizes of 1 μm^2, were in contact with the alumina ball in the pin-on-disk tests. Friction forces were measured here as a function of normal force

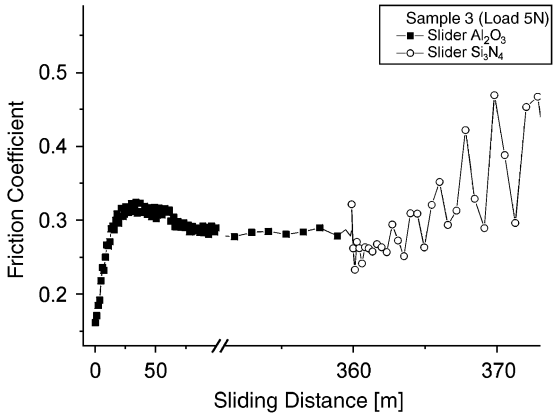

Fig. 2. Coefficient of friction as a function of sliding distance measured using various balls. μ was measured with an α-Al_2O_3 ball for 360 m. After sliding for 360 m, the ball was exchanged against a Si_3N_4 ball (load 5 N, velocity 0.05 m/s, 40% RH, 25°C). RH, relative humidity.

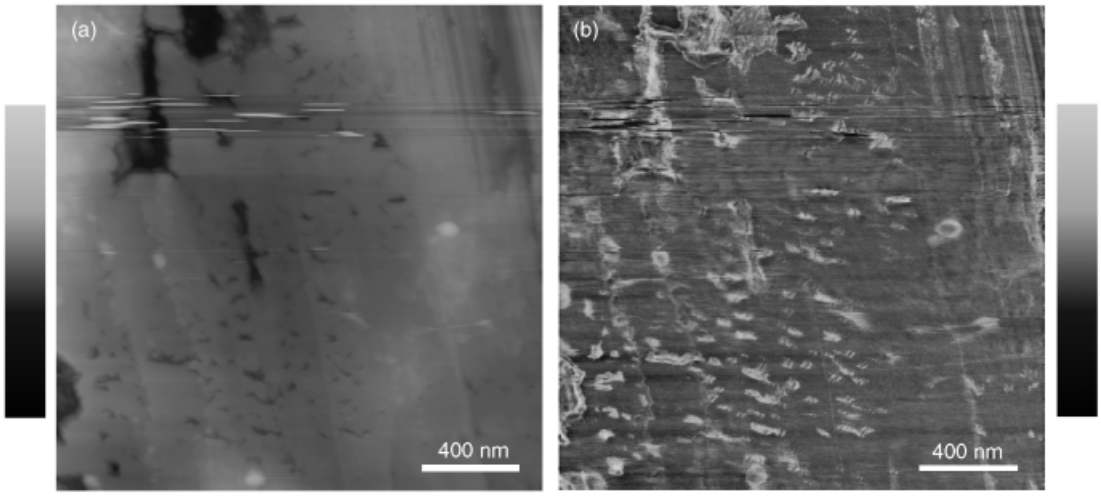

Fig. 3. Contact mode atomic force microscopic images of wear track C (300 m) using a Si_3N_4 tip: (a) topography, the height (z) scale covers height differences of 100 nm from dark to bright; (b) friction force map, the vertical scale covers friction differences of 40 nN from dark to bright (load 0 nN, adhesion force 22.6±1.2 nN, velocity 6.1 μm/s, 40% RH, 25°C). RH, relative humidity.

in the wear-less, elastic contact regime (onset of yielding: 3.6 GPa) using Si_3N_4 as the probe (tip) material. The same environmental conditions were maintained as for the pin-on-disk experiment (40% RH and 25°C).

A linear increase of the friction force with increasing normal forces was observed in the range of applied normal forces (see Supporting Information, Figure S2). There was no hysteresis for the data acquired with increasing and decreasing loads. The average contact pressure of 1.2 GPa, calculated using the Hertz mode (assuming sphere–flat contact, a maximum applied load of 25 nN, an AFM tip radius of 70 nm, Young's modulii of 150 and 130 GPa, and Poisson's ratios of 0.25 and 0.3 for the tip and the sample), was in the same range as the values in the macrotribology test (1 GPa). However, the tip–sample contact length of ~7 nm (for a tip with a radius of 70 nm) was significantly smaller as compared with 100–200 μm in the pin-on-disk experiments for a ball with a radius of 5 mm.

The coefficient of friction was determined from the slope of a linear least-squares fit. Data acquired in different locations of similar morphological appearance were found to show consistent results (Table I).

The coefficients of friction measured on wear tracks A and B after 20 and 30 m of sliding were significantly higher than the value for the area outside the wear tracks. After longer sliding distances (track C, 300 m), the coefficient of friction decreased to a value of 0.30.

As revealed in the macrotribology test, the surface layer of the sample (contamination and/or a thin soft layer that may be generated during polishing) is removed by wear during the initial sliding in the pin-on-disk test. Thus, the areas in the track probed subsequently by AFM may possess different properties as compared with areas outside the track, resulting in different values of the coefficient of friction. Moreover, the low-friction behavior disappeared after O_2-plasma treatment of the samples subsequent to the pin-on-disk test (see Table II); the coefficient of friction of plasma-treated wear track (300 m sliding distance) increased nearly by a factor of 1.5. By contrast, the modification by the O_2-plasma did not affect $\mu^{nano}_{Si_3N_4}$ for the other areas to within the experimental error. These observations may indicate that the surface composition of track C was indeed different from the other tracks and the outside area.

Because all components of the sample are in the highest oxidation state (ZrO_2, Y_2O_3, and CuO), as concluded from XPS measurements (data not shown), oxidation of the surface may be excluded. By contrast, sputtering and the concomitant roughening of the top layer of material in track C by the O_2-plasma treatment are a more plausible explanation for this surface modification. Thus, these results support the notion that,

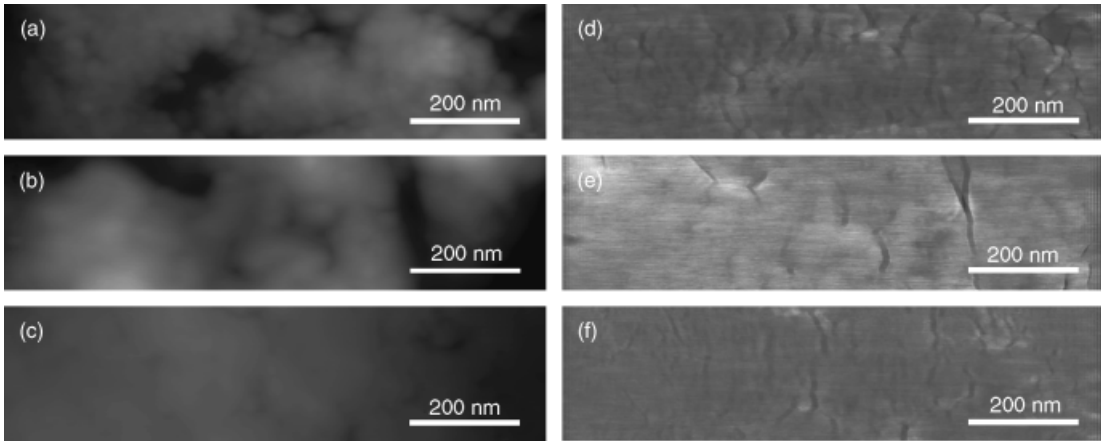

Fig. 4. Contact mode atomic force microscopic images of wear tracks in a yttria-stabilized tetragonal zirconia (3Y-TZP) sample doped with 8 mol% CuO (after sliding with an α-Al_2O_3 ball for different distances in a pin-on-disk tribometer) using a Si_3N_4 tip ((a)–(c) topography and (d)–(f) corresponding friction maps, for sliding distances of: (a, d) 20 m (track A), (b, e) 30 m (track B), and (c, f) 300 m (track C), compare Fig. 1). The height scale in (a)–(c) covers height differences of 100 nm from dark to bright; the vertical scale in (d)–(f) covers friction differences of 30 nN from dark to bright (load 0 nN, adhesion force (d) 12±2 nN, (e) 13.5±1.5 nN, and (f) 22.6±1.2 nN, velocity 6.1 μm/s, 40% RH, 25°C). RH, relative humidity.

Table I. Coefficient of Friction Measured on Wear Tracks and Areas Outside the Tracks Determined at Different Locations of Sample 1 Using a Si_3N_4 Tip (Velocity 6.1 μm/s, 40% RH, 25°C)

Location #	Outside tracks	Track A, sliding distance 20 m	Track B, sliding distance 30 m	Track C, sliding distance 300 m
1	0.50	0.73	0.91	0.29
2	0.55	0.81	0.80	0.25
3	0.49	0.63	0.86	0.37
Average value $\mu^{nano}_{Si_3N_4}$	0.51	0.72	0.85	0.30
Standard deviation	0.03	0.08	0.06	0.03

RH, relative humidity.

during sliding, an interfacial layer with low shear strength was generated.

The velocity dependence of $\mu^{nano}_{Si_3N_4}$ was determined using the recently described high-velocity AFM accessory.[6] Velocities approaching the values used in the pin-on-disk experiments were obtained. Figure 5 shows the coefficient of friction as a function of velocity for track D (sliding distance of 100 m) measured with a Si_3N_4 tip. In the range of the attainable velocities (between 6 and 500 μm/s), $\mu^{nano}_{Si_3N_4}$ was found to be *independent* of velocity. Higher velocities were inaccessible due to too high sample mass and sample roughness (see also Tocha *et al.*[6]). Similarly, for oxidized Si(100) and nanostructured zirconia, no dependence of $\mu^{nano}_{Si_3N_4}$ on velocity was found in the range of 10 μm/s to 1 mm/s.[6] These data are also qualitatively in agreement with macrotribology experiments where the coefficient of friction for the 3Y-TZP doped with CuO was also found to be independent of velocity in the range of 0.05–0.5 m/s.[22]

It is assumed that the coefficient of friction will also be independent of velocities for the range of velocities between those that can be probed by AFM and those that can be accessed by pin-on-disk experiments (i.e., between 5×10^2 and 5×10^4 μm/s). Based on this assumption, the values obtained on the nanometer scale with a velocity of 6–500 μm/s can be directly compared with the values measured using the pin-on-disk tribometer with 5×10^4 μm/s.

(3) Comparative Discussion of Macro- and Nanotribology on CuO-Doped 3Y-TZP

The comparison of the macro- and nanotribological data of the soft interfacial layer formed in the wear track is based on the assumption that, in the absence of wear, $\mu^{macro}_{Si_3N_4}$ and $\mu^{macro}_{\alpha\text{-}Al_2O_3}$ are very similar. Thus, $\mu^{nano}_{Si_3N_4}$ and $\mu^{macro}_{\alpha\text{-}Al_2O_3}$ can be directly compared, as shown in Fig. 6 for various sliding distances.

As expected, the areas outside the wear tracks deviate significantly for different samples. The value of $\mu^{nano}_{Si_3N_4}$ of 0.70–0.85 measured in these areas was significantly higher compared with $\mu^{macro}_{\alpha\text{-}Al_2O_3}$ of 0.33. It was also higher than that measured for undoped 3Y-TZP ($\mu^{nano}_{Si_3N_4} = 0.5$). However, for long sliding distances (>100 m), very similar values of $\mu^{macro}_{\alpha\text{-}Al_2O_3}$ and $\mu^{nano}_{Si_3N_4}$ were observed.

Table II. Coefficient of Friction $\mu^{nano}_{Si_3N_4}$ of the Sample Analyzed Directly after Pin-on-Disk Measurements without any Additional Treatment, and the Sample Analyzed after Pin-on-Disk Test and Subsequent Modification for 10 min in an O_2-Plasma

$\mu^{nano}_{Si_3N_4}$	No treatment	Modified by O_2-plasma
Track A	0.72±0.08	0.86±0.10
Track B	0.85±0.06	0.81±0.15
Track C	0.30±0.03	0.47±0.04

The measurements were performed with a Si_3N_4 tip using AFM (velocity 6.1 μm/s, 40% RH, 25°C). AFM, atomic force microscopy; RH, relative humidity.

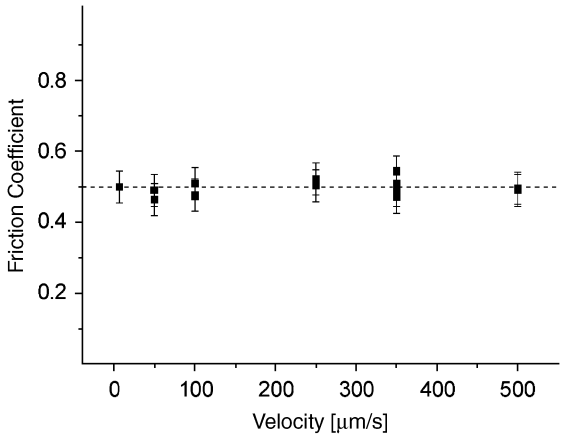

Fig. 5. Coefficient of friction versus velocity for track D (sliding distance of 100 m) measured with the Si_3N_4 tip using the high-velocity atomic force microscope described in Tocha *et al.*[6] (40% RH, 25°C). RH, relative humidity.

For short sliding distances of 20–30 m, the smooth areas analyzed on the nanometer scale are regions where the contamination layer was removed in the pin-on-disk test and the highest asperities were worn. Because the areas probed did not show local variations in friction force, it can be concluded that the generated layer in these regions is continuous already for these short sliding distances. The soft layer in these areas is very thin and the contact is dominated by the contact of the AFM tip (single/few asperity) with the underlying 3Y-TZP; see Fig. 7. By contrast, the large-scale multiasperity contact of the alumina ball in the pin-on-disk experiments on this heterogeneous and rough sample is already dominated by the contact of the ball with the soft layer. Consequently, we observe $\mu^{nano} > \mu^{macro}$ for measurements on wear tracks with short sliding distances.

Longer sliding distances resulted in values of nanometer scale coefficient of friction comparable to the values measured on the micrometer scale. This result is consistent with a layer thickness in those smooth areas that is sufficient to provide low-friction behavior for the single/few asperity contact (Fig. 7(b)). In addition, the modification of the surface of track C using O_2-plasma treatment (Table II), which caused a significant increase of the coefficient of friction after treatment, suggests a surface chemical difference between those tracks (presence of the soft layer on a track of 300 m sliding distance). For a long sliding distance of 450 m (track F), $\mu^{nano}_{Si_3N_4}$ is slightly higher than $\mu^{macro}_{\alpha\text{-}Al_2O_3}$. The increase in the coefficient of friction can be due to different reasons: (i) an increase in layer thickness above the critical value, resulting in a coefficient of friction similar to the bulk value of the layer material used or (ii) wear of the soft layer, accompanied by a significant increase in roughness. In addition, one may consider tribochemistry to be the origin of the observed changes; however, we do not possess any experimental evidence for this possible explanation at this point.

The first situation (i) is predicted by the model for layer thickness above 1 μm.[25] The second case (ii) was observed experimentally for the macroscopic coefficient of friction for sliding distances above 1000 m. Because the roughness of track for 300 and 450 m sliding distances (tracks E and F) was practically the same, we can exclude (ii) as a reason for the increase in $\mu^{nano}_{Si_3N_4}$ with respect to $\mu^{macro}_{\alpha\text{-}Al_2O_3}$. Most probably, the higher coefficient of friction is caused by an increase in the layer thickness, as described by the model (Fig. 7(c)). However, the critical layer thickness for this single/few asperity contact may be thinner than the value calculated for rough surfaces.

The excellent agreement between $\mu^{nano}_{Si_3N_4}$ and $\mu^{macro}_{\alpha\text{-}Al_2O_3}$ for sliding distances of 100–300 m shown above could be a coincidence, because the values of $\mu^{nano}_{Si_3N_4}$ are most likely overestimated due to humidity effects. As described in Tocha *et al.*[36], the coefficient of friction as determined by AFM was observed to depend

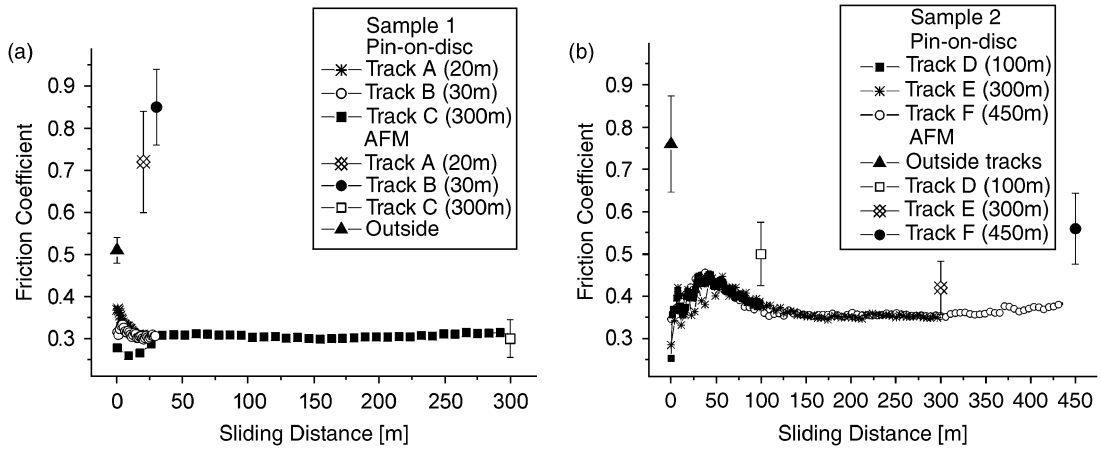

Fig. 6. Comparison of nano- and macrotribology for two individual CuO-doped yttria-stabilized tetragonal zirconia (3Y-TZP) specimens. Coefficients of friction versus sliding distance measured by atomic force microscopy using Si_3N_4 tips and by a pin-on-disk tribometer against an α-Al_2O_3 ball (40% RH, 25°C). RH, relative humidity.

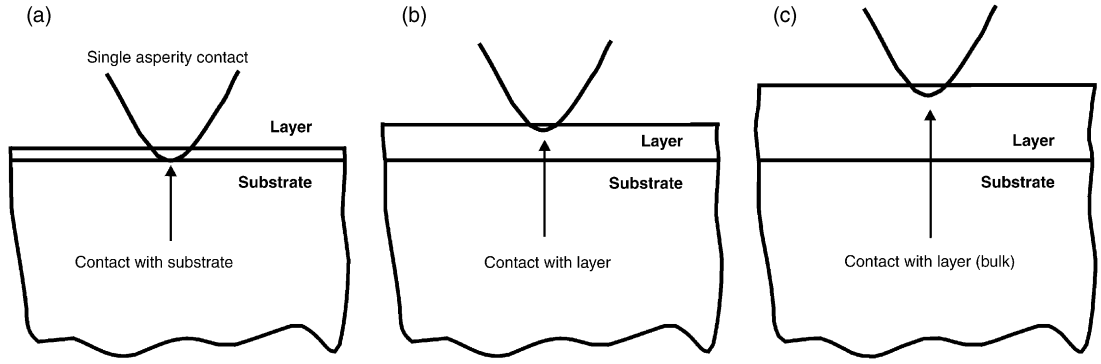

Fig. 7. Schematic of a single asperity contact with a layered system for different layer thickness: (a) a thin layer, (b) a layer with intermediate thickness, and (c) a thick layer (bulk).

critically on the RH. For nanostructured ZrO_2, an increase in μ^{nano} by a factor of 2 was observed when the RH was changed from $<5\%$ (dry nitrogen conditions) to 40% RH. This increase was attributed to the action of capillary forces in a humid environment. The maximum coefficient of friction was observed for a value of 40% RH. By contrast, differences in the coefficient of friction as a function of humidity in macrotribology are small.[26] Hence, the real $\mu^{nano}_{Si_3N_4}$ of the smooth areas (in the absence of capillary forces) is very likely smaller than $\mu^{macro}_{\alpha\text{-}Al_2O_3}$. A lower value of the coefficient of friction would in fact be expected for friction in the absence of ploughing (μ^{nano}) as compared with the normal friction (μ^{macro}).[1]

IV. Conclusions

In this paper, complementary nano- and macrotribology measurements of CuO-doped 3Y-TZP ceramics were reported. Using quantitative nanotribology analysis and our newly developed high-velocity AFM accessory,[5,6] the gap between nano- and macrotribology in terms of length and time scales was considerably narrowed. In particular, the effect of velocity on the coefficient of friction and a soft layer formation during sliding on different length scales were studied. The observed trends in the coefficient of friction determined on the nanometer scale by AFM are in agreement with the data acquired using a pin-on-disk tribometer on the micrometer scale. During the initial sliding in pin-on-disk experiments the layer of surface contaminations is removed and wear of high asperities occurs. For sliding distances >100 m, very similar values of $\mu^{macro}_{\alpha\text{-}Al_2O_3}$ (which we assume to be of similar value of $\mu^{macro}_{Si_3N_4}$) and $\mu^{nano}_{Si_3N_4}$ were observed. This observation may indicate that during sliding an interfacial layer with low shear strength is generated and that the AFM measurements were performed on this layer. While these results do not provide a complete explanation for the process of layer formation, they represent the first report of bridged nano- and macrotribological analysis of a compositionally heterogeneous low-friction, low-wear ceramic material, and confirm some of the key assumptions for the model by Pasaribu and Schipper.[24,25]

Acknowledgments

The authors thank Dr. S. Ran, Dr. A. J. A. Winnubst, and Prof. D. H. A. Blank (IMS group, University of Twente, the Netherlands) for the preparation of the ceramic samples.

References

[1]E. Meyer, R. M. Overney, K. Dransfeld, and T. Gyalog, *Nanoscience Friction and Rheology on the Nanometer Scale*. World Scientific, Singapore, 1998.
[2]R. W. Carpick and M. Salmeron, "Scratching the Surface Fundamental Investigations of Tribology with Atomic Force Microscopy," *Chem. Rev.*, **97**, 1163–94 (1997).
[3]H. Czichos, "Tribology and Its Many Facets From Macroscopic to Microscopic and Nano-Scale Phenomena," *Meccanica*, **36**, 605–15 (2001).
[4]I. Iordanoff, Y. Berthier, S. Descartes, and H. Heshmat, "A Review of Recent Approaches for Modeling Solid Third Bodies," *J. Tribol.—Trans. ASME*, **124**, 725–35 (2002).
[5]E. Tocha, H. Schönherr, and G. J. Vancso, "Quantitative Nanotribology by AFM: A Novel Universal Calibration Platform," *Langmuir*, **22**, 2340–50 (2006).
[6]E. Tocha, T. Stefañski, H. Schönherr, and G. J. Vancso, "Development of a High Velocity Accessory for Atomic Force Microscopy-Based Friction Measurements," *Rev. Sci. Instrum.*, **76**, 083704 (2005).
[7]H. Czichos, D. Klaffke, E. Santner, and M. Woydt, "Advances in Tribology: The Materials Point of View," *Wear*, **190**, 155–61 (1995).
[8]N. J. Fox, B. Tyrer, and G. W. Stachowiak, "Boundary Lubrication Performance of Free Fatty Acids in Sunflower Oil," *Tribol. Lett.*, **16**, 275–81 (2004).
[9]H. E. Sliney, "Solid Lubricant Materials for High Temperatures—A Review," *Tribol. Int.*, **15**, 303–15 (1982).

[10]F. P. Bowden and D. Tabor, *Friction and Lubrication of Solids, Part I.* Clarendon Press, Oxford, 1950.
[11]M. Chhowalla and G. A. J. Amaratunga, "Thin Films of Fullerene-Like MoS_2 Nanoparticles with Ultra-Low Friction and Wear," *Nature*, **407**, 164–7 (2000).
[12]C. Grossiord, J. M. Martin, T. Le Mogne, and T. Palermo, "UHV Friction of Tribofilms Derived from Metal Dithiophosphates," *Tribol. Lett.*, **6**, 171–9 (1999).
[13]J. Koskinen, H. Ronkainen, J. P. Hirvonen, R. Lappalainen, and K. A. Pischow, "Characterization of the Mechanical Properties of Carbon Metal Multilayered Film," *Diam. Relat. Mater.*, **4**, 843–7 (1995).
[14]L. Rapoport, Y. Bilik, Y. Feldman, M. Homyonfer, S. R. Cohen, and R. Tenne, "Hollow Nanoparticles of WS_2 as Potential Solid-State Lubricants," *Nature*, **387**, 791–3 (1997).
[15]I. L. Singer, "Mechanics and Chemistry of Solids in Sliding Contact," *Langmuir*, **12**, 4486–91 (1996).
[16]B. L. Vlcek, B. L. Sargent, and J. L. Lauer, "Lubrication of Ceramic Contacts by Surface-Deposited Pyrolytic Carbon," *Lubric. Eng.*, **49**, 463–71 (1993).
[17]B. Kerkwijk, M. Garcia, W. E. van Zyl, L. Winnubst, E. J. Mulder, D. J. Schipper, and H. Verweij, "Friction Behaviour of Solid Oxide Lubricants as Second Phase in Alpha-Al_2O_3 and Stabilised ZrO_2 Composites," *Wear*, **256**, 182–9 (2004).
[18]N. M. Renevier, N. Lobiondo, V. C. Fox, D. G. Teer, and J. Hampshire, "Performance of MoS_2/Metal Composite Coatings Used for Dry Machining and Other Industrial Applications," *Surf. Coat. Technol.*, **123**, 84–91 (2000).
[19]N. Alexeyev and S. Jahanmir, "Mechanics of Friction in Self-Lubricating Composite-Materials. 1. Mechanics of 2nd-Phase Deformation and Motion," *Wear*, **166**, 41–8 (1993).
[20]N. Alexeyev and S. Jahanmir, "Mechanics of Friction in Self-Lubricating Composite-Materials. 2. Deformation of the Interfacial Film," *Wear*, **166**, 49–54 (1993).
[21]Y. Wang, F. J. Worzala, and A. R. Lefkow, "Friction and Wear Properties of Partially-Stabilized Zirconia with Solid Lubricant," *Wear*, **167**, 23–31 (1993).
[22]H. R. Pasaribu, J. W. Sloetjes, and D. J. Schipper, "Friction Reduction by Adding Copper Oxide into Alumina and Zirconia Ceramics," *Wear*, **255**, 699–707 (2003).
[23]A. J. A. Winnubst, S. Ran, K. W. Wiratha, D. H. A. Blank, H. R. Pasaribu, J. W. Sloetjes, and D. J. Schipper, "Wear-Resistant Zirconia Ceramic for Low Friction Application," *Eur. Ceram. VIII, Parts 1–3*, **264–268**, 809–12 (2004).
[24]H. R. Pasaribu, "Friction and Wear of Zirconia and Alumina Ceramics Doped with CuO"; Ph.D. Thesis, University of Twente, Enschede, the Netherlands, 2005.
[25]H. R. Pasaribu and D. J. Schipper, "Deterministic Friction Model of a Rough Surface Sliding Against a Flat Layered Surface," *Tribol. Lett.*, **17**, 967–76 (2004).
[26]H. R. Pasaribu, K. M. Reuver, D. J. Schipper, S. Ran, K. W. Wiratha, A. J. A. Winnubst, and D. H. A. Blank, "Environmental Effects on Friction and Wear of Dry Sliding Zirconia and Alumina Ceramics Doped with Copper Oxide," *Int. J. Refract. Met. Hard Mater.*, **23**, 386–90 (2005).
[27]S. Ran, L. Winnubst, W. Wiratha, and D. H. A. Blank, "Sintering Behavior of 0.8 mol%-CuO-Doped 3Y-TZP Ceramics," *J. Am. Ceram. Soc.*, **89**, 151–5 (2006).
[28]M. Tortonese and M. Kirk, "Characterization of Application-Specific Probes for SPMs," *Proc. SPIE*, **3009**, 53–60 (1997).
[29]U. D. Schwarz, O. Zwörner, P. Köster, and R. Wiesendanger, "Quantitative Analysis of the Frictional Properties of Solid Materials at Low Loads. 1. Carbon Compounds," *Phys. Rev. B*, **56**, 6987–96 (1997).
[30]U. D. Schwarz, O. Zwörner, P. Köster, and R. Wiesendanger, "Quantitative Analysis of the Frictional Properties of Solid Materials at Low Loads. 2. Mica and Germanium Sulfide," *Phys. Rev. B*, **56**, 6997–7000 (1997).
[31]J. A. Hammerschmidt, W. L. Gladfelter, and G. Haugstad, "Probing Polymer Viscoelastic Relaxations with Temperature-Controlled Friction Force Microscopy," *Macromolecules*, **32**, 3360–7 (1999).
[32]D. F. Ogletree, R. W. Carpick, and M. Salmeron, "Calibration of Frictional Forces in Atomic Force Microscopy," *Rev. Sci. Instrum.*, **67**, 3298–306 (1996).
[33]M. Varenberg, I. Etsion, and G. Halperin, "An Improved Wedge Calibration Method for Lateral Force in Atomic Force Microscopy," *Rev. Sci. Instrum.*, **74**, 3362–7 (2003).
[34]H. R. Pasaribu and D. J. Schipper, "Application of a Deterministic Contact Model to Analyze the Contact of a Rough Surface Against a Flat Layered Surface," *J. Tribol. Trans. ASME*, **127**, 451–5 (2005).
[35]I. L. Singer, S. D. Dvorak, K. J. Wahl, and T. W. Scharf, "Role of Third Bodies in Friction and Wear of Protective Coatings," *J. Vac. Sci. Technol. A*, **21**, S232–40 (2003).
[36]E. Tocha, N. Siebelt, H. Schönherr, and G. J. Vancso, "Influence of Grain Size and Humidity on the Nanotribological Properties of Wear-Resistant Nanostructured ZrO_2 Coatings An Atomic Force Microscopy Study," *J. Am. Ceram. Soc.*, **88**, 2498–503 (2005).

Supplementary Material

The following supplementary material is available for this article online:

Fig. S1. Left: SEM image of various wear tracks; right: XPS intensity profiles for various elements recorded between points 5 and 44 indicated in the SEM micrograph. In the position of the wear track the C1s signal is significantly reduced, in agreement with a removal of carbon-containing contaminations in the pin on disc test.

Fig. S2. Friction force (calibrated difference photodiode output signal) versus normal force data for track B (30 m) measured in 40% RH at 25°C with velocity of 6.1 m/s; the error bars indicate the standard deviation (n = 128) of the data analyzed for a given normal force.

This material is available as part of the online article from: http://www.blackwell-synergy.com/doi/abs/10.1111/j.1551-2916.2008.02334.x (This link will take you to the article abstract).

Please note: Blackwell Publishing are not responsible for the content or functionality of any supplementary materials supplied by the authors. Any queries (other than missing material) should be directed to the corresponding author for the article. □